

N₄O₃ Heptadentate Dinuclear ZnII complex show Catalytic Catecholase Activity in Mixed Aqueous Solution

Amar Hens*

Assistant Professor, Dept Of Chemistry, G.G.D.C. At Ranibandh, Bankura, Govt. Of West Bengal, India.

Corresponding Author: Amar Hens*

Abstract : The model Zinc II dinuclear complex was highly active in catalyzing the aerobic oxidation of 3,5-di-tert-butylcatechol (3,5-DTBC) to 3,5-di-tert-butylbenzoquinone (3,5-DTBQ) in mixed aqueous solution at pH 8.5, the activity measured in terms of k_{cat} is 4.58 min^{-1} with very high catalytic efficiency (k_{cat}/K_M) 3.3×10^6 . Saturation kinetic studies show that the order of conversion of substrate to product quinone has been confirmed by UV-vis spectrophotometric study.

Keywords: Heptadentate ligand, dinuclear complex, crystal structure, DFT study, catecholase activity

Date of Submission: 12-11-2017

Date of acceptance: 30-11-2017

I. Introduction

Catechol oxidase (CO), mainly found in plant tissues and crustaceans, copper III types catalyzes are responsible for the oxidation of a wide range of o-diphenols (catechols) to the corresponding o-quinones [1]. In general quinones are highly reactive compounds and readily undergo an autopolymerization leading to formation of melanin. The catechol to quinone conversion is not only important in biological system but also it has a great utility towards in medical diagnosis. In medical science it mainly use for the determination of the hormonally active catecholamines adrenaline, noradrenaline, and dopa [2]. In modern research field mainly focused on the synthetic analogues of catechol oxidase in bioinorganic chemistry to understand the in-depth functional mechanisms of catechol oxidase and elucidate different internal and external factors which may influence the activity [3].

From all the previous observations, we concluded that redox-active metal ions such as CuII, MnII, MnIII catalyze the reaction based on the mechanism in a metal-centred redox pathway, while redox-inactive metal ion such as ZnII takes a radical pathway [4] for the same reaction. Although there are a few scattered reports of the interactions of catechol model substrates with zinc-based systems [5], a mechanism has only been revealed in a single report with Schiff-base compartmental ligand system [6-8]. Here in we synthesized a unique dinuclear Zn (II) complex are prone to catalyze the oxidation of 3,5-di-tert-butylcatechol (3,5-DTBC) to 3,5-di-tert-butylbenzoquinone (3,5-DTBQ) in mixed aqueous solution at pH 8.5. Here we also present a systematic study of the oxidation of Catecholase activity using the complex as a catalyst.

Here, we also present a full density functional theory (DFT) and time-dependent density functional theory (TDDFT) to get better insight into the geometry of these systems. Geometry optimization of the singlet ground-state was carried out by means of DFT calculations. Solution state optimized geometry revealed that the inter metallic distance take an important role to find out the oxidation process of 3,5-di-tert-butylcatechol (3,5-DTBC) to 3,5-di-tert-butylbenzoquinone (3,5-DTBQ).

II. Experimental Section

2.1 Materials

All the starting chemicals were analytically pure and used without further purification.

Caution! Perchlorate salts are highly explosive, and should be handled with care and in small amounts.

2.2 Physical measurements

The molar conductivity was determined using Systronics Conductivity Meter 304 in acetonitrile solution at room temperature. Elemental analyses (C, H, N) were performed on Perkin-Elmer 2400 series II analyzer. UV-Vis spectra were recorded on a Perkin-Elmer LAMBDA 25 spectrophotometer.

2.3 Computational details

The geometrical structure of the complex **1** [Zn₂L₂H₂O] was optimized by the DFT [9] method with B3LYP exchange correlation functional [10] approach. The geometry of the complex was fully optimized in solution phase without any symmetry constraints. The vibrational frequency calculation was also performed for

the complex to ensure that the optimized geometry represents the local minima and there are only positive eigen values. The effective core potential (ECP) approximation of Hay and Wadt was used for describing the (1s²2s²2p⁶) core electron for zinc whereas the associated “double- ξ ” quality basis set LANL2DZ was used for the valence shell [11]. For H atoms, we used 6–31+G basis set and for C, N and O atoms, we employed 6–31+G* as basis set to optimize the ground state geometry. All the calculations were performed with the Gaussian 09W software package [12]. Gauss Sum 2.1 program [13] was used to calculate the molecular orbital contributions from groups or atoms.

Table 1 Crystal data and structure refinement parameters for [Zn₂L·2H₂O]·H₂O·ClO₄.

	1·H₂O·ClO₄
Formula	C ₃₁ H ₄₇ ClN ₄ O ₁₀ Zn ₂
M _r	801.96
Crystal system	Monoclinic
Space group	P21/c
a / Å	12.599(4)
b / Å	24.548(7)
c / Å	12.890(4)
α / °	90
β / °	115.528(2)
γ / °	90
V / Å ³	3597.7(2)
Z	4
D _{calcd} / mg m ⁻³	1.473
μ / mm ⁻¹	1.466
θ / °	1.7- 27.5
T / K	293(2)
Reflns collected	8253
R1, ^a wR2 ^b [I > 2 σ (I)]	0.058, 0.150
GOF on F ²	1.008

$$^a R1 = \sum | |F_o| - |F_c| | / \sum |F_o|, \quad ^b wR2 = [\sum [w(F_o^2 - F_c^2)^2] / \sum [w(F_o^2)^2]]^{1/2}.$$

2.4 Crystallographic studies

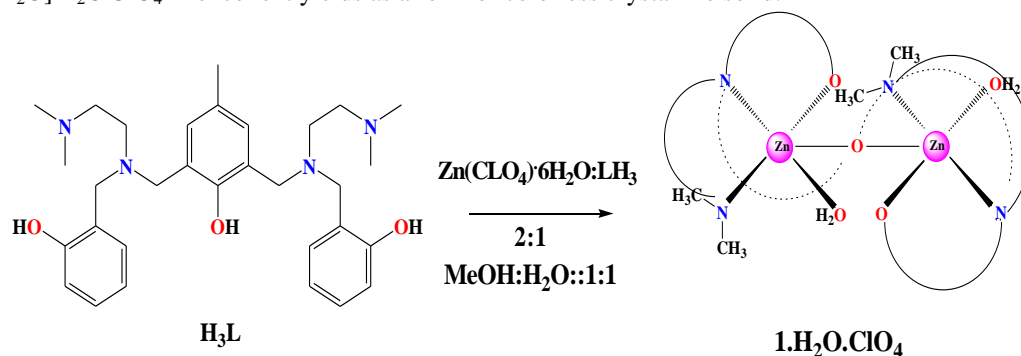
The single crystal suitable for X-ray crystallographic analysis of the complex **1·H₂O·ClO₄**, [Zn₂L·2H₂O]·H₂O·ClO₄ was obtained by slow evaporation of aqua-methanolic solution. The X-ray intensity data were collected on Bruker AXS SMART APEX CCD diffractometer (Mo K α , λ = 0.71073 Å) at 293 K. The detector was placed at a distance 6.03 cm from the crystal. Total 606 frames were collected with a scan width of 0.3° in different settings of ϕ . The data were reduced in SAINTPLUS [14] and empirical absorption correction was applied using the SADABS package [14]. Metal atom was located by Patterson Method and the rest of the non-hydrogen atoms emerged from successive Fourier synthesis. The structure was refined by full matrix least-square procedure on F². All non-hydrogen atoms were refined anisotropically. All calculations were performed using the SHELXTL V 6.14 program package [15]. Molecular structure plots were drawn using the ORTEP [16a] and Mercury [16b] software. Relevant crystal data are given in Table 1.

2.5 Synthesis of complex

1·H₂O·ClO₄, [Zn₂L·2H₂O]·H₂O·ClO₄ An aqueous solution of Zn(ClO₄)₂·6H₂O (0.230 g, 0.60 mM) was added to a methanolic solution of H₃L (0.150 g, 0.29 mM) and the reaction mixture was warmed in water bath with care. A dilute methanolic solution of Et₃N (0.090 g, 0.90 mM) was then added to the reaction mixture to maintain at a pH of 7-8; then refluxed for 2 hours with afforded air and was allowed to cool to room temperature. The reaction mixture was then filtered, and the volume of solvent was reduced via rotary evaporator to obtain a white residue. The residue was filtered and washed by methanol and was then dried in vacuum. Colorless single crystals suitable for diffraction were obtained from water-methanol (1:4) mixture. Yield: 0.210 g (88%). Elemental Anal. Calcd. for C₃₁H₄₇ClN₄O₁₀Zn₂: C, 46.43; H, 5.91; N, 6.99. Found: C, 46.39; H, 5.92; N, 7.01. ¹H NMR { δ (ppm) ar = aromatic, Me (N) = amine- methyl, Me (C) = aromatic- methyl, Bz =benzyl, My = methylene}: 7.41 (H10, ar), 7.22 (H2, ar), 7.19 (H3, ar), 7.01 (H4, ar), 3.88 (H7, Bz), 3.8 (H10, Bz), 2.75 (H8, My), 2.55 (H9, My), 2.33 (H27, Me(N)) and 2.19 (H29, Me(C)). ESI-MS (CH₃CN): m/z Calcd. 647.1730, Found: 647.1784 (100%). Molar conductance, Λ_M : (CH₃CN solution) 126 Ω^{-1} cm² mol⁻¹.

III. Result And Discussion

The heptadentate symmetrical N₄O₃ ligand H₃L is react with Zn(ClO₄)₂·6H₂O in a ratio of 1:2 in methanol and water mixture at room temperature in air produces complexes of composition [Zn₂L·2H₂O]·H₂O·ClO₄ in excellent yields as a form of colorless crystalline solid.



Scheme 1 Schematic representation for the synthesis of **1a**·H₂O·ClO₄.

3.1 Crystal structure of [Zn₂L·2H₂O]·H₂O·ClO₄

The asymmetric unit of complex **1**·H₂O·ClO₄ contains one L³⁻, two Zn²⁺ ions, three water molecules and one perchlorate anion (Fig. 4a). The geometry around the Zn1 atom is distorted trigonal bipyramidal ($\tau = 0.75$) whereas that of Zn2 is intermediate between square based pyramid and distorted trigonal bipyramid ($\tau = 0.43$) [17]. The binuclear core comprises of two zinc atom bridged equatorially by endogenous cresolate group. The equatorial positions at Zn1 are occupied by O1 and O2 atoms of phenoxo group, N2 atom of amine group and the axial positions are occupied by N1 of atom of amine and O4 of the coordinated water molecule respectively. Similarly the equatorial base of Zn2 is formed by O2, O3 and N4 atoms and the axial positions are occupied by N3 and O5 atoms. Both zinc centers are surrounded by pentacoordinated identical environment of N₂O₃ donor in which the Zn–O and Zn–N bond distances vary between 1.968(3)–2.121(5) Å and 2.113(4)–2.131(4) Å, respectively (Table 2). The axial angle of two zinc centers O4–Zn1–N1 and O5–Zn2–N3 are 171.15(15)° and 168.83(16)°. The larger deviation from 180° is observed in Zn2 moiety preferred the square based pyramidal shape. The Zn···Zn separation in the complex is 3.455 Å. In the complex, one uncoordinated water molecule is also present per formula unit (Fig. 1).

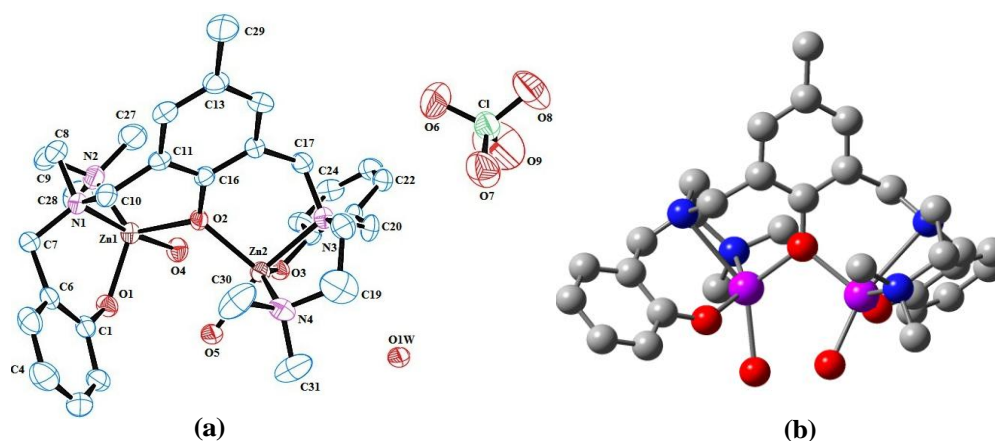


Fig. 4 (a) Asymmetric unit of complex **1**·H₂O·ClO₄ with displacement ellipsoids drawn at the 25% probability level and hydrogen atoms have been omitted for clarity; (b) Optimized molecular structures of **1**, in methanol. (Zn: Pale violet, N: Blue, O: Red, C: Grey. Hydrogen atoms are omitted for clarity).

3.2 Geometry optimization in solution phase and ground state analysis

The geometry optimization of **1** was performed in solution phase (methanol) and the significant bond distances of the optimized geometry of this at their ground S₀ state along with the crystal structure parameter was given in Table 2. The optimized structure was shown in Fig. 1b. In solution phase the geometry around the Zn1 atom is intermediate between square based pyramid and distorted trigonal bipyramid ($\tau = 0.34$) whereas that of Zn2 is square based pyramid ($\tau = 0.07$) [17].

Table 2 Selected Bond Lengths (Å) for **1**·H₂O·ClO₄ and Selected Optimized Geometrical Parameters of complexes **1** in the Ground (S₀) State at B3LYP Levels in methanol.

Bond length (Å)					
Atoms (Zn1)	Solid state	Soln. state	Atoms (Zn2)	Solid state	Soln. state
Zn1-O1	1.968(3)	1.97832	Zn2-O2	2.024(3)	2.08980
Zn1-O2	2.023(3)	2.11592	Zn2-O3	1.999(3)	2.00004
Zn1-O4*	2.121(5)	2.3341	Zn2-O5*	2.063(4)	2.31819
Zn1-N1	2.131(4)	2.20961	Zn2-N3	2.116(4)	2.25998
Zn1-N2	2.113(4)	2.21772	Zn2-N4	2.114(4)	2.18427

* The oxygen atom is coordinated water molecule.

The crystal structure data (Table 2) is in good agreement with optimized parameters and the discrepancy (maximum deviation 0.255 Å for Zn2-O5 bond distance and 0.143 Å for Zn2-N3) comes from the crystal lattice distortion existing in real molecules. In each bond length some relaxation arises in solution phase which leads larger bond distance and influenced the bond angle as well as changes the geometrical environment over the zinc metal. It was remarkably observed that the maximum deviation arises at Zn1-O4 and Zn2-O5 bond distance in solution phase. The lengthening of bond distance of zinc ion with oxygen atom of coordinated water molecule in solution phase implies that the displacement of water molecule in solution phase. The Zn^{II}Zn separation of the complex in solution state was 3.201 Å, which implies that in solution state two zinc atoms come closer to each other. This close proximity among the two metal nuclei in solution phase is responsible for its catalytic behavior [18].

3.3 Catechol Oxidase Activity of the complex.

In order to confirm the ability of the zinc(II) complex to oxidize 3,5-DTBC, 1 × 10⁻⁴ mol dm⁻³ methanolic solution was treated with 1.5 × 10⁻² mol dm⁻³ (150 equiv) of 3,5-DTBC under aerobic conditions. The course of the reaction was followed by UV-vis spectroscopy, and the time-dependent spectral scan of the complex is depicted in Fig. 3b. Initially, pH-dependent studies were carried out to determine the pH value at which catecholase activity reached a maximum. The influence of pH on the reaction rate for oxidation of 3,5-DTBC catalyzed by complex was determined over the pH range of 5.5–9.0 at 25 °C (Fig. 2a).

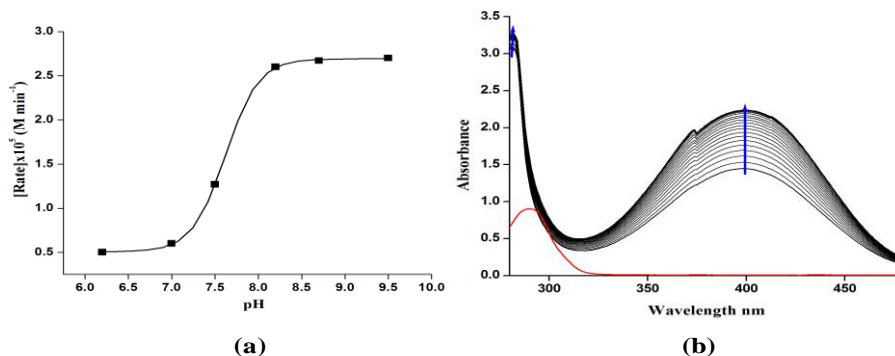


Fig. 2. (a) Dependence of the initial reaction rates on pH for the oxidation of 3,5-DTBC catalyzed by complex 1. (b) Time dependent growth of 3,5-DTBQ at 400 nm in methanol, 25 °C.

The buffers used were MES (2-(N-morpholino)ethanesulfonic acid, pH 6.0–6.5), HEPES (4-(2-hydroxyethyl)piperazine-1-ethanesulfonic acid, pH 7.0–8.5) and TRIS (tris(hydroxymethyl) aminomethane, pH 9.0–9.5). Since a hump was clearly obtained at pH 8.0, detailed studies with the complex have been continued in this pH. The reaction was monitored for 1.5 h after addition of 3,5-DTBC to the methanolic solution of the complex. Initially, complex does not show any absorbance band at 400 nm. Upon addition of 3,5-DTBC the spectral run done immediately exhibits increment of the absorbance nearly above that band. Since it is well established that 3,5-DTBQ shows band maxima at 400 nm in pure methanol, the experiment unequivocally proves oxidation of 3,5-DTBC to 3,5-DTBQ catalyzed by the dinuclear Zn(II) complex. The kinetics of the 3,5-DTBC oxidation was determined by monitoring the increase of the product 3,5-DTBQ. The increase in the concentration of quinone with when time catalyzed by complex is plotted in Fig. 2b.

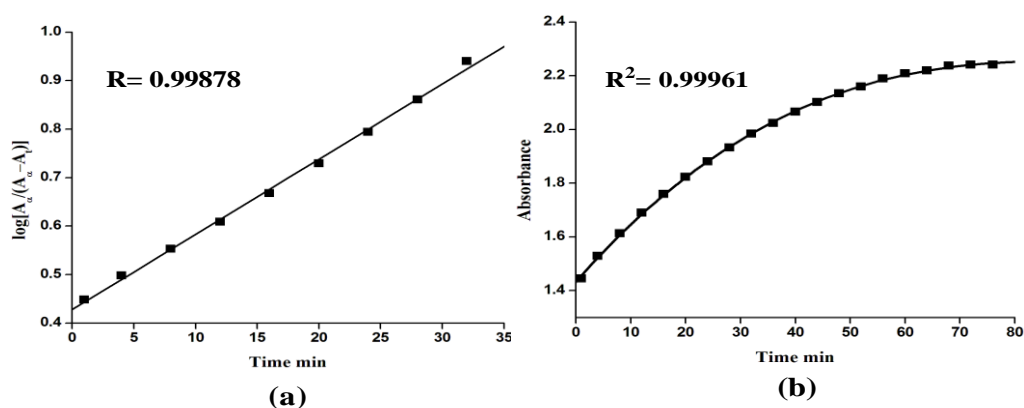


Fig. 3. (a) The nature of initial reaction rate of catalytic reaction. (b) Plot of concentration of 3,5-DTBQ vs time.

Table 3 Kinetic Parameter of dinuclear Zn(II) catalyst.

V_{max}	K_M	$k_c \text{ min}^{-1}$
16.03×10^{-5}	8×10^{-5}	4.58

The kinetic study of the oxidation of 3,5-DTBC to 3,5-DTBQ by the complexes was carried out by monitoring the increase of absorption of quinone at 400 nm by the initial rate (V_0) method. There is a linear relationship between the initial rate and the concentration of the substrate indicating the first order dependence on the 3,5-DTBC concentration for this system (Fig. 3a). Saturation kinetics were found for the initial rates versus the 3,5-DTBC concentration for the complexes and are shown in Fig. 3b. The complex showed saturation kinetics where a treatment based on the Michaelis–Menten model seemed to be appropriate. The values of the Michaelis binding constant (K_m), maximum velocity (V_{max}), and rate constant for dissociation of substrates (i.e., turnover number, k_{cat}) were calculated for complexes from the graphs of $1/V$ vs $1/[S]$ (Fig. 4b), known as the Lineweaver–Burk graph using the equation $1/V = \{KM/V_{max}\} \{1/[S]\} + 1/V_{max}$, and the kinetic parameters are presented in Table 3.

In the electronic spectra, the complexes exhibit an intraligand charge transfer band in 240 nm (high energy) and a ligand to metal charge transfer band at 290 nm (low energy) which is probably due to $PhO^-Zn(II)$.

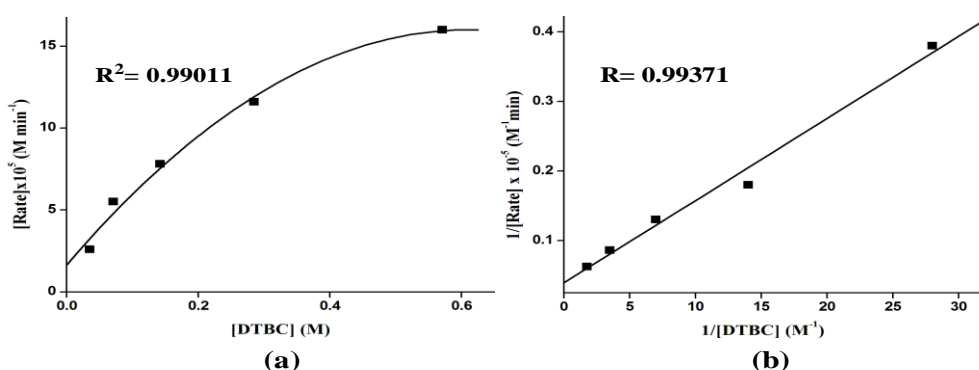
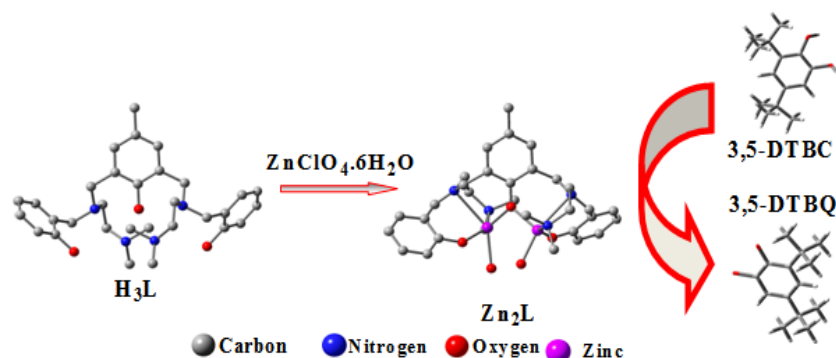


Fig. 4. (a) Dependence of the initial reaction rates on the 3,5-DTBC concentration for the oxidation reaction catalyzed by Zn (II) complex. (b) Lineweaver-Burk plot for aerobic oxidation of 3,5-DTBC by complex.

On addition of 3,5-DTBC solution to the solution of the maintaining 150:1 molar ratio (Fig. 3a) followed by spectral scan shows generation of a new bands at 400 along with retaining of the band at ~285 nm (Fig. 2b). The intensity of all those three bands is observed to increase gradually with time. The formation of bands at ~285 and their gradual increment with time indicate that phenoxo radical species are most probably forming during catalysis.



Scheme 1. A Schematic representation of the catecholase oxidation activity by the dinuclear ZnII complex.

IV. Conclusion

In conclusion, a simple and low cost heptadentate N_4O_3 coordinating, p-cresol and salicylaldehyde based dinuclear zinc complex was synthesized. The synthesized complex has been found to be excellent catalytic activity towards 3,5-di-tert-butylcatechol (3,5-DTBC) under aerobic condition.

Acknowledgements

Amar Hens acknowledge UGC, New Delhi, India. The valuable discussion and help of Prof. Kajal Krishna Rajak, Dept. of Chemistry, Jadavpur University, Kolkata, is kindly acknowledged. The author also acknowledge to the Department of Chemistry, Govt. General Degree College Ranibandh, Bankura (Govt. of West Bengal).

References

- [1]. R. Than, A. A. Feldmann and B. Krebs, Structural and functional studies on ... and catechol oxidases, *Coord. Chem. Rev.* 182, 1999, 211-215.
- [2]. S. Torelli, C. Belle, I. Gautier-Luneau, J. L. Pierre, E. Saint-Aman, J. M. Latour, L. Le Pape and D. Luneau, pH controlled change of the metal coordination in dicopper..., *Inorg. Chem.* 39, 2000, 3526-3536.
- [3]. E. Monzani, L. Quinti, A. Perotti, L. Casella, M. Gullotti, L. Randaccio, S. Geremia, G. Nardin, P. Faleschini and G. Tabbi, Tyrosinase Models. Synthesis, Structure, Catechol Oxidase Activity, and Phenol Monooxygenase Activity of a Dinuclear Copper Complex Derived from a Triamino Pentabenzimidazole Ligand, *Inorg. Chem.* 37, 1998, 553-562.
- [4]. A. Guha, T. Chattopadhyay, N. D. Paul, M. Mukherjee, S. Goswami, T. K. Mondal, E. Zangrando and D. Das, Radical pathway in catecholase activity with zinc-based model complexes of compartmental ligands, *Inorg. Chem.*, 51, 2012, 8750-8759.
- [5]. (a) M. E. Bodini, G. Copia, R. Robinson and D. T. Sawyer, Designed metalloprotein stabilizes a semiquinone radical, *Inorg. Chem.*, 22, 1983, 126-129; (b) A. Hens, A. Maity and K. K. Rajak, N, N coordinating schiff base ligand acting as a fluorescence sensor for zinc (II) and colorimetric sensor for copper (II), and zinc (II) in mixed aqueous media *Inorg. Chimica Acta.*, 423, 2014, 408-420.
- [6]. (a) A. Hens, *RSC Adv.*, 5, 2015, 54352-54363; (b) A. Hens, B. N. Seal *J. Sc.* 7, 2016, 35-38.
- [7]. A. Hens, P. Mondal and K. K. Rajak, *Dalton Trans.*, 42, 2013, 14905-14915.
- [8]. P. Mondal, A. Hens, S. Basak, and K. K. Rajak, *Dalton Trans.*, 42, 2013, 1536-1549.
- [9]. (a) E. Runge and E. K. U. Gross, *Phys. Rev. Lett.* 52, 1984, 997; (b) A. Hens and K. K. Rajak, *J. Ind. Chem. Soc.* 92, 2015, 1805-1815; (c) A. Hens, P. Mondal and K. K. Rajak, *Polyhedron*, 85, 2015, 255-266.
- [10]. (a) A. D. Becke, *J. Chem. Phys.* 98, 1993, 5648; (b) C. Lee, W. Yang and R. G. Parr, *Phys. Rev. B.*, 37, 1988, 785-789; (c) A. Hens and K. K. Rajak, *RSC Adv.* 5, 2015, 44764-44777.
- [11]. (a) P. J. Hay and W. R. Wadt, *J. Chem. Phys.* 82, 1985, 299-310; (b) R. L. Martin, *J. Chem. Phys.*, 118, 2003 4775-4777.
- [12]. M. J. Frisch, G. W. Trucks, H. B. Schlegel, G. E. Scuseria, M. A. Robb, J. R. Cheeseman, G. Scalmani, V. Barone, B. Mennucci, G. A. Petersson, H. Nakatsuji, M. Caricato, X. Li, H. P. Hratchian, A. F. Izmaylov, J. Bloino, G. Zheng, J. L. Sonnenberg, M. Hada, M. Ehara, K. Toyota, R. Fukuda, J. Hasegawa, M. Ishida, T. Nakajima, Y. Honda, O. Kitao, H. Nakai, T. Vreven, J. A. Montgomery Jr., J. E. Peralta, F. Ogliaro, M. Bearpark, J. J. Heyd, E. Brothers, K. N. Kudin, V. N. Staroverov, R. Kobayashi, J. Normand, K. Raghavachari, A. Rendell, J. C. Burant, S. S. Iyengar, J. Tomasi, M. Cossi, N. Rega, J. M. Millam, M. Klene, J. E. Knox, J. B. Cross, V. Bakken, C. Adamo, J. Jaramillo, R. Gomperts, R. E. Stratmann, O. Yazyev, A. J. Austin, R. Cammi, C. Pomelli, J. W. Ochterski, R. L. Martin, K. Morokuma, V. G. Zakrzewski, G. A. Voth, P. Salvador, J. J. Dannenberg, S. Dapprich, A. D. Daniels, Ö. Farkas, J. B. Foresman, J. V. Ortiz, J. Cioslowski, D. J. Fox, *Gaussian 09*, (Revision A.1) Gaussian, Inc., Wallingford, CT, 2009.
- [13]. (a) N. M. O'Boyle, A. L. Tenderholt and K. M. Langner, *J. Comp. Chem.*, 29, 2008 839-845.
- [14]. SMART; SAINT; SADABS; XPREP; SHELXTL, Bruker AXS Inc., Madison, WI, 1998.
- [15]. G. M. Sheldrick, SHELXTL, v. 6.14, Bruker AXS Inc., Madison, WI, 2003.

- [16]. (a) C. K. Johnson, ORTEP Report ORNL-5138, Oak Ridge National Laboratory, Oak Ridge, TN, 1976; (b) C.F. Macrae, P.R. Edgington, P McCabe, E. Pidcock, G.P. Shields, R. Taylor, M. Towler and J. van de Streek, *J. Appl. Cryst.*, 39, 2006, 453-.
- [17]. J. W. Geary, *Coord. Chem. Rev.*, 7, 1971, 81-122.
- [18]. R. Sanyal, S. K. Dash, S. Das, S. Chattopadhyay, S. Roy, D. Das, *J Biol Inorg Chem.*, 19, 2014, 1099-1111.

Amar Hens N₄O₃ Heptadentate Dinuclear ZnII complex show Catalytic Catecholase Activity in Mixed Aqueous Solution.” *IOSR Journal of Applied Chemistry (IOSR-JAC)*, vol. 10, no. 11, 2017, pp. 30-36.